Cell Host & Microbe
Article

The Second Messenger Phosphatidylinositol-5-Phosphate Facilitates Antiviral Innate Immune Signaling

Takumi Kawasaki,[1,2,4] Naoki Takemura,[2,4,5] Daron M. Standley,[3] Shizuo Akira,[2,4,*] and Taro Kawai[1,2,4,*]
[1]Laboratory of Molecular Immunobiology, Graduate School of Biological Sciences, Nara Institute of Science and Technology (NAIST), 8916-5 Takayama, Ikoma, Nara 630-0192, Japan
[2]Laboratory of Host Defense, WPI Immunology Frontier Research Center
[3]Laboratory of Systems Immunology, WPI Immunology Frontier Research Center
[4]Department of Host Defense, Research Institute for Microbial Diseases
Osaka University, Osaka 565-0871, Japan
[5]Division of Innate Immune Regulation, International Research and Development Center for Mucosal Vaccines, Institute of Medical Science, The University of Tokyo, Tokyo 108-8639, Japan
*Correspondence: sakira@biken.osaka-u.ac.jp (S.A.), tarokawai@bs.naist.jp (T.K.)
http://dx.doi.org/10.1016/j.chom.2013.07.011

SUMMARY

Innate immune receptors, notably Toll-like receptors (TLRs) and RIG-I-like receptors (RLRs), sense viral infection and activate transcription factors, including interferon regulatory factor-3 (IRF3), to induce type I interferon (IFN). We demonstrate that the lipid phosphatidylinositol-5-phosphate (PtdIns5P) is increased upon viral infection and facilitates type I IFN production by binding to IRF3 and its upstream kinase TBK1 and promoting TBK1-mediated IRF3 phosphorylation and activation. Additionally, we determine that PtdIns5P is produced through the kinase PIKfyve, which phosphorylates PtdIns to generate PtdIns5P. Accordingly, PIKfyve knockdown or pharamoclogical inhibition decreases PtdIns5P levels and type I IFN production after TLR or RLR stimulation, and results in increased viral replication. A synthetic PtdIns5P, C8-PtdIns5P, promotes IRF3 phosphorylation and cytokine production in dendritic cells and acts as an adjuvant to boost immune responses in immunized mice. Thus, PtdIns5P produced during viral infection is a second messenger that targets the TBK1-IRF3 axis to elicit antiviral immunity.

INTRODUCTION

Detection of pathogen components and subsequent induction of innate immune responses, such as the production of inflammatory cytokines and type I interferon (IFN), is mediated by pattern-recognition receptors (PRRs), including Toll-like receptors (TLRs), RIG-I-like receptors (RLRs), C-type lectin receptors, NOD-like receptor,rs and intracellular sensors for DNA (AIM2, DAI, DDX41, LRRFIP1, MRE11, and cGAS) (Kawai and Akira, 2011; Kondo et al., 2013; Sancho and Reis e Sousa, 2012; Strowig et al., 2012; Sun et al., 2013). These receptors trigger intracellular signaling pathways that lead to the coordinated activation of several transcription factors, including members of the interferon regulatory factor (IRF) and NF-κB families. Among these, IRF3 controls expression of IFNβ and other cytokine genes during viral and bacterial infection. In the steady state, IRF3 is localized in the cytoplasm and translocates to the nucleus by forming a dimer after viral infection or stimulation with bacterial lipopolysaccharide (LPS). IRF3 activation is initiated by phosphorylation of serine and threonine clusters in its C terminus by the serine/threonine kinases TANK-binding kinase 1 (TBK1) and IκB kinase i (IKKi) (Fitzgerald et al., 2003).

The TBK1-IRF3 axis is activated by multiple stimuli and plays critical roles in the induction of type I IFN (Honda et al., 2006). TLR3 and TLR4, which recognize viral double-stranded (ds) RNA and LPS, respectively, activate TBK1 and IRF3 through an adaptor, TRIF. RLRs are composed of RIG-I and MDA5, which sense RNA species from various RNA viruses. RLRs recruit an adaptor protein, IPS-1 (also known as MAVS, Cardif, or VISA), and eventually activate TBK1-IRF3 signaling. The TBK1-IRF3 axis is also involved downstream of STING, is required for induction of the cytosolic DNA-mediated type I IFN-inducing pathway, and was shown to be essential for DNA vaccine-induced innate and adaptive immune responses (Ishii et al., 2008). However, the detailed mechanisms of how the TBK1-IRF3 axis is regulated remain unclear.

Phosphatidylinositol (PtdIns) lipids regulate a variety of biological responses, including signal transduction, organelle trafficking, cytoskeletal regulation, and innate immune responses. PtdIns4P, produced by the kinase PI4KIIIα, is required for hepatic virus C entry and replication (Berger and Randall, 2009). PtdIns3,4,5P_3 has been proposed to regulate innate immune signaling (Koyasu, 2003). Deficiency of the p85α subunit of PI3K, which generates PtdIns3,4,5P_3, enhances NF-κB activation through AKT and GSK3β and increases cytokine production. Deficiency of PTEN, a PtdIns3,4,5P_3 phosphatase, leads to constitutively enhanced PI3K signaling activity. PtdIns3P from PI3K binds to the $p40^{phox}$ and $p47^{phox}$ oxidase complex and enhances reactive oxygen production for bacterial defense (Koyasu, 2003). Contributions of PI3K in IRF3- and IRF7-mediated innate immune signaling have been discussed (Guiducci et al., 2008; Hrincius et al., 2011). It was shown that

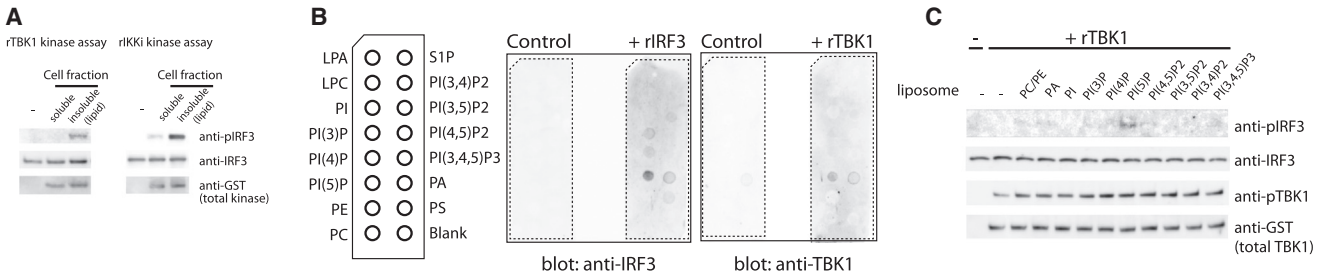

Figure 1. PtdIns5P Enhances IRF3 Phosphorylation by TBK1 In Vitro

(A) Fractionated cellular components were subjected to in vitro kinase assay by incubation with recombinant IRF3 (rIRF3) and TBK1 (rTBK1) (left) or IKKi (rIKKi) (right), and IRF3 phosphorylation was detected by an anti-pS394IRF3 antibody.

(B) Lipid interactions with IRF3 (left) or TBK1 (right) were detected by protein lipid overlay assay.

(C) PE/PC-based liposomes with the indicated synthetic C16-PtdIns were subjected to in vitro kinase assay by incubation with rIRF3 and rTBK1. Figure 1 is related to Figure S1.

Shigella flexneri inject PtdIns4,5P_2-4-phosphatase into host cells to increase cellular PtdIns5P production, which supports their survival (Pendaries et al., 2006).

Here, we screened cellular components and identified PtdIns5P as a facilitator of TBK1-mediated IRF3 phosphorylation. PtdIns5P is produced from PIKfyve, which phosphorylates the phosphatidylinositol ring at the 5′ position. Intracellular levels of PtdIns5P were increased in mammalian cells after dsRNA stimulation and viral infection. PtdIns5P directly bound to IRF3 and caused IRF3 activation by facilitating IRF3 phosphorylation via TBK1. Notably, synthetic water-soluble C8-PtdIns5P acted as an agonist of the TBK1–IRF3 axis and enhanced adaptive immune responses in vivo. Taken together, these findings suggest that PtdIns5P is a second messenger in antiviral innate immune signaling.

RESULTS

Identification of PtdIns5P

To identify cellular components that regulate the TBK1-IRF3 axis, we set up an in vitro screening system. We prepared recombinant TBK1 and IRF3, and these were mixed with various reagents in the presence of ATP. After the in vitro kinase reaction, we detected IRF3 activation by immunoblotting using an antibody against S396-phosphorylated IRF3. We incubated TBK1 and IRF3 together with DMXAA (a vascular disrupting agent that activates STING), dsDNA (poly[dA:dT]), high KCl concentration, H_2O_2, or recombinant STING, but none of these enhanced IRF3 phosphorylation (see Figure S1A online and data not shown). We then tested whether cellular components participated in IRF3 phosphorylation. To this end, we separated HEK293T cells into water-soluble and -insoluble fractions using chloroform/methanol. The water-insoluble fraction (chloroform layer), which contains lipids or cholesterol, was dried and resuspended in reaction buffer. The water-insoluble fraction increased IRF3 phosphorylation by TBK1 and IKKi (Figure 1A). Moreover, the water-insoluble fraction isolated from HEK293T cells transfected with IPS-1 strongly induced IRF3 phosphorylation, compared with controls (Figure S1B), indicating that lipids enriched in activated cells are responsible for TBK1-mediated IRF3 activation.

To further identify the lipids involved in IRF3 activation, we screened lipids bound to TBK1 or IRF3 using a protein lipid overlay (PLO) assay. TBK1 bound to PtdIns5P, and IRF3 bound to several anionic lipids including PtdIns5P (Figure 1B). No binding of these proteins to cationic or other lipids was detectable (data not shown). This suggests that phosphatidylinositols can promote IRF3 phosphorylation in vitro. To examine the involvement of these phosphatidylinositols in IRF3 activation, various synthetic phosphatidylinositols were mixed with phosphatidylcholine (PC) and phosphatidylethanolamine (PE) to form liposomes and subjected to the in vitro kinase assay. Among the phosphatidylinositols, PtdIns5P-containing liposomes facilitated IRF3 phosphorylation (Figure 1C). Overexpression of TBK1 caused autoactivation of TBK1 (Clark et al., 2009). Therefore further increase of TBK1 phosphorylation at S172 might not be observed (Figure 1C). TBK1 phosphorylation was not increased in in vitro kinase assay using endogenous TBK1 precipitated from RAW264.7 cells (Figure S1C), suggesting that TBK1 phosphorylation at S172 was not affected by PtdIns5P.

Identification of PIKfyve

We next sought to identify the kinases or phosphatases responsible for production of PtdIns5P during viral infection (Figure 2A). To this end, HEK293 cells were transfected with an expression plasmid for the candidate genes together with an IFN-stimulated response element (ISRE) reporter plasmid, and luciferase expression was measured by reporter assay. Luciferase expression increased with overexpression of PIKfyve, a kinase that synthesizes PtdIns5P or PtdIns3,5P_2 by phosphorylation of position 5 in the inositol ring (Figure S2A). Previous studies using overexpression of PIKfyve or cells deficient for PIKfyve demonstrated that PIKfyve mediates PtdIns5P production (Ikonomov et al., 2011; Sbrissa et al., 2002). PIKfyve is a 250 kDa protein containing a fyve domain and a kinase domain. We found that protein and mRNA level of PIKfyve expression were increased with poly(I:C) (synthetic analog of dsRNA recognized by TLR3 or RLRs), poly(dA:dT) and RNA virus, and Newcastle disease virus (NDV) stimulation, but not by LPS stimulation (Figure S2B). Overexpression of PIKfyve in HEK293 cells increased ISRE and IFNβ promoter activity but did not influence NF-κB promoter activity (Figure 2B). In contrast, a kinase-negative mutant of

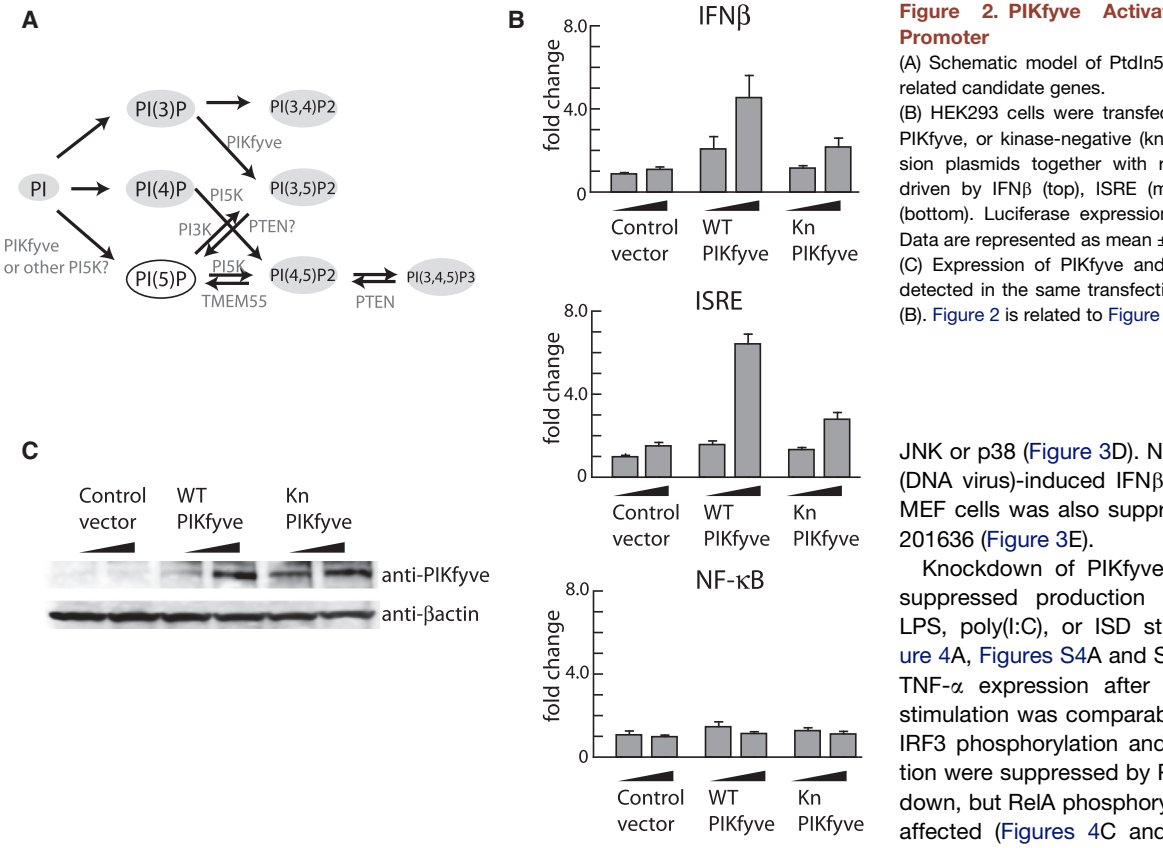

Figure 2. PIKfyve Activates the IFNβ Promoter

(A) Schematic model of PtdIn5P generation and related candidate genes.

(B) HEK293 cells were transfected with control, PIKfyve, or kinase-negative (kn) PIKfyve expression plasmids together with reporter plasmids driven by IFNβ (top), ISRE (middle), or NF-κB (bottom). Luciferase expression was measured. Data are represented as mean ± SD.

(C) Expression of PIKfyve and kn PIKfyve was detected in the same transfection condition with (B). Figure 2 is related to Figure S2.

PIKfyve (kn PIKfyve) failed to activate these promoters upon overexpression. Expression levels were comparable between wild-type and kinase-negative PIKfyve, suggesting that mutation of PIKfyve at K1831M did not affect the protein stability (Figure 2C). These results suggested that PtdIns5P production by PIKfyve regulates IFNβ production.

Roles of PIKfyve in the TBK1-IRF3 Axis Signaling Pathway

To address whether PIKfyve regulates antiviral innate immune responses, we utilized YM-201636, a PIKfyve inhibitor (Jefferies et al., 2008). Expression of IFNβ mRNA induced by LPS, poly(I:C), and DNA was abrogated by YM-201636 treatment in mouse embryonic fibroblast (MEF) cells (Figure 3A). IFNβ and IP-10 production was suppressed by YM-201636 in a dose-dependent manner (Figure S3A), but LPS- and R837 (TLR7 ligand)-induced TNF-α production in GM-CSF-induced bone marrow-derived dendritic cells (GM-DCs) was not affected (Figure S3B). To clarify the signaling pathway, we quantified NF-κB activity by ELAM-luciferase and IRF activity by ISRE-luciferase in HEK293 cells (Figure 3B). ISRE activation by LPS, poly(I:C), and poly(dA:dT) stimulation was suppressed, but NF-κB activation was not. In addition, IRF3 phosphorylation after stimulation with LPS, poly(I:C) or interferon stimulatory DNA (ISD) (synthetic dsDNA) was suppressed by YM-201636 treatment in GM-DCs, but phosphorylation of RelA, a member of the NF-κB family, was not affected (Figure 3C and Figure S3C). Furthermore, YM-201636 treatment suppressed IRF3 dimer formation in response to poly(I:C) but did not influence phosphorylation of JNK or p38 (Figure 3D). NDV and HSV-1 (DNA virus)-induced IFNβ expression in MEF cells was also suppressed by YM-201636 (Figure 3E).

Knockdown of PIKfyve in MEF cells suppressed production of IFNβ after LPS, poly(I:C), or ISD stimulation (Figure 4A, Figures S4A and S4B). However, TNF-α expression after LPS or R837 stimulation was comparable (Figure 4B). IRF3 phosphorylation and dimer formation were suppressed by PIKfyve knockdown, but RelA phosphorylation was not affected (Figures 4C and 4D and Figure S4C). JNK and p38 phosphorylation were also not affected (Figure S4D). In addition, NDV- and HSV-1-dependent IFNβ production and IRF3 phosphorylation were also abrogated by PIKfyve knockdown in MEF cells (Figure 4E) and GM-DCs (Figures S4E and S4F). Virus titers of NDV were increased by PIKfyve knockdown in MEF cells (Figure 4F). Reduction of IRF3 activity by PIKfyve knockdown was also supported by a luciferase assay in HEK293 cells (Figure 4G, Figures S4G–S4I). Collectively, these results suggest that PIKfyve is required for the TBK1-IRF3 axis activation in innate immune signaling.

Increased PtdIns5P Production in Innate Immune Signaling

PtdIns5P production is increased by several stimuli (Wilcox and Hinchliffe, 2008), and PIKfyve appears to be the main source for production of PtdIns5P, suggested by analyses of gene-deficient mice (Ikonomov et al., 2011). We measured PtdIns5P levels in MEF cells by the PtdIns5P mass assay. Radioactive-labeled lipids were separated by TLC (Figure 5A, left), and the intensities measured by densitometry were plotted as a bar graph (Figure 5A, right). Production of PtdIns5P increased upon stimulation with poly(I:C), LPS, or infection with NDV (Figures 5A and B). H_2O_2 was used as a positive control (Jones et al., 2006). To confirm that poly(I:C)-induced PtdIns5P production is dependent on PIKfyve, PtdIns5P production was measured after YM-201636 treatment or PIKfyve knockdown (Figures 5C and 5D). Time course experiments indicated that production of PtdIns5P increased to peak levels at 15 min after poly(I:C) stimulation and decreased gradually thereafter. However, cells pretreated with

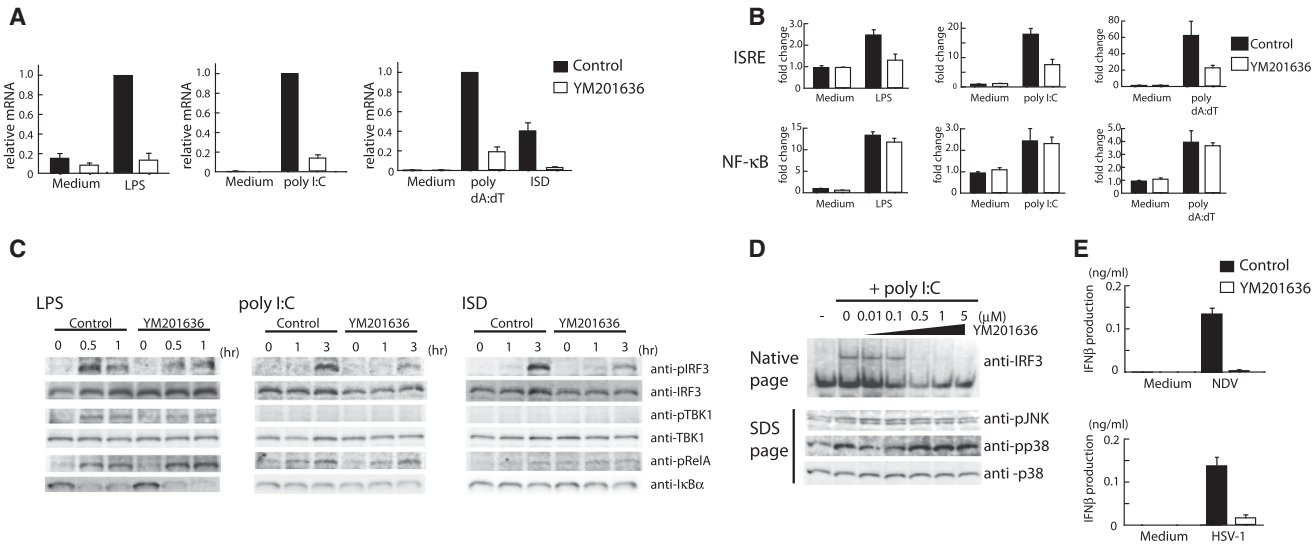

Figure 3. PIKfyve Kinase Inhibitor Suppresses IFNβ Production

(A) MEF cells pretreated with 0.5 μM YM-201636 for 30 min were stimulated with LPS, poly(I:C), poly(dA:dT), or ISD transfection, and expression of IFNβ mRNA was measured by qPCR.

(B) HEK293 cells pretreated with YM-201636 were stimulated with LPS, poly(I:C), or poly(dA:dT). Activation of ISRE and NF-κB promoter was measured by luciferase assay. HEK293-expressing TLR4/MD2/CD14 cells were used for LPS stimulation.

(C) GM-DCs were stimulated with LPS or transfected with poly(I:C) and ISD, and immunoblotting was performed with the indicated antibodies.

(D) IRF3 dimer formation was detected by native-PAGE analysis (top), and p38 and JNK phosphorylation were detected by SDS-PAGE followed by immunoblotting (bottom).

(E) MEF cells were infected with NDV (top) or HSV-1 (bottom) after treatment with YM-201636. IFNβ production was measured by ELISA. Data are represented as mean ± SD. Figure 3 is related to Figure S3.

YM-201636 failed to show increased PtdIns5P production (Figure 5C). Similarly, knockdown of PIKfyve abrogated poly(I:C)-induced PtdIns5P production (Figure 5D). Although PtdIns5P mainly accumulated in the nucleus in the steady state (Jones et al., 2006), PIKfyve localized in the cytosol and endosome-like structures in MEF cells (Figure 5E) (Rutherford et al., 2006). PIKfyve in endosome-like structures only partially colocalized with STING or other endosome markers (Figure 5E), and localization of PIKfyve did not dramatically change after poly(I:C), LPS, or DNA stimulation (data not shown). Although the localization of PIKfyve is not clear, PtdIns5P production after poly(I:C) in the cytosol was three times higher than basal levels (Figure 5F). However, PtdIns5P production in the nucleus was almost comparable. These results suggest that increase of cytosolic PtdIns5P produced from PIKfyve is important for regulation of the TBK1-IRF3 axis. Although mechanisms of how PIKfyve activity is controlled are not clear, one possibility is that the binding of PIKfyve to IPS-1 and TRIF induces PIKfyve activation (Figure 5G).

PtdIns5P Binds the LRH Pocket of IRF3

Autophosphorylation of TBK1 at S172 was reported to be linked to its activation (Clark et al., 2009; Kishore et al., 2002), but phosphorylation at S172 was not inhibited by PIKfyve inhibitor or knockdown (Figure 3C, Figures S3C and S4C). In addition, TBK1 phosphorylation after LPS or R837 stimulation was clearly observed, but not by poly(I:C) or ISD stimulation, which is consistent with a recent study (Figure 3C and Figure S3C) (Clark et al., 2011). These results suggested that increased phosphorylation and activation of TBK1 are not always related to IRF3 phosphorylation. Furthermore, the in vitro kinase assay demonstrated that addition of PtdIns5P did not induce detectable enhancement of TBK1 phosphorylation (Figure 1C, Figures S1B and S1C). These findings suggest that TBK1 is not a critical target for PtdIns5P in terms of IRF3 activation.

Next, we examined whether IRF3 association with PtdIns5P was important for its regulation. Based on the human IRF3 structure, several clusters of anionic amino acids at the surface of IRF3 were proposed to be a regulatory domain and may bind electrostatically to PtdIns5P (Qin et al., 2003; Takahasi et al., 2003). We investigated IRF3-PtdIns5P interactions by PLO assay using recombinant hIRF3 containing anionic amino acids replaced by Ala. The K360A/R361A mutation of hIRF3 had a lower affinity for PtdIns5P than wild-type IRF3 (Figure 6A). In addition, the K360A/R361A mutant did not induce PtdIns5P-dependent IRF3 phosphorylation at S396 in vitro (Figure 6B). The cellular functional role of K360/R361 was tested by the rescue of wild-type or mutant murine IRF3 in *Irf3*$^{-/-}$ MEF cells. K352/R353 (homologous amino acid to K360/R361 in hIRF3) in mIRF3 is critical for phosphorylation, dimer formation (Figure 6C), and cytokine gene expression (Figure 6D and Figure S5A). These results collectively suggested that the PtdIns5P interaction with K360/R361 in hIRF3 is important for TBK1-IRF3 axis activation. In addition to IRF3 phosphorylation, we also examined whether PtdIns5P from PIKfyve could regulate the interaction between TBK1 and IRF3. HEK293T cells were cotransfected with IRF3 and TBK1 or TBK1 kinase negative (kn), and cells were treated with YM-201636 (Figure 6E). TBK1-IRF3 interactions were

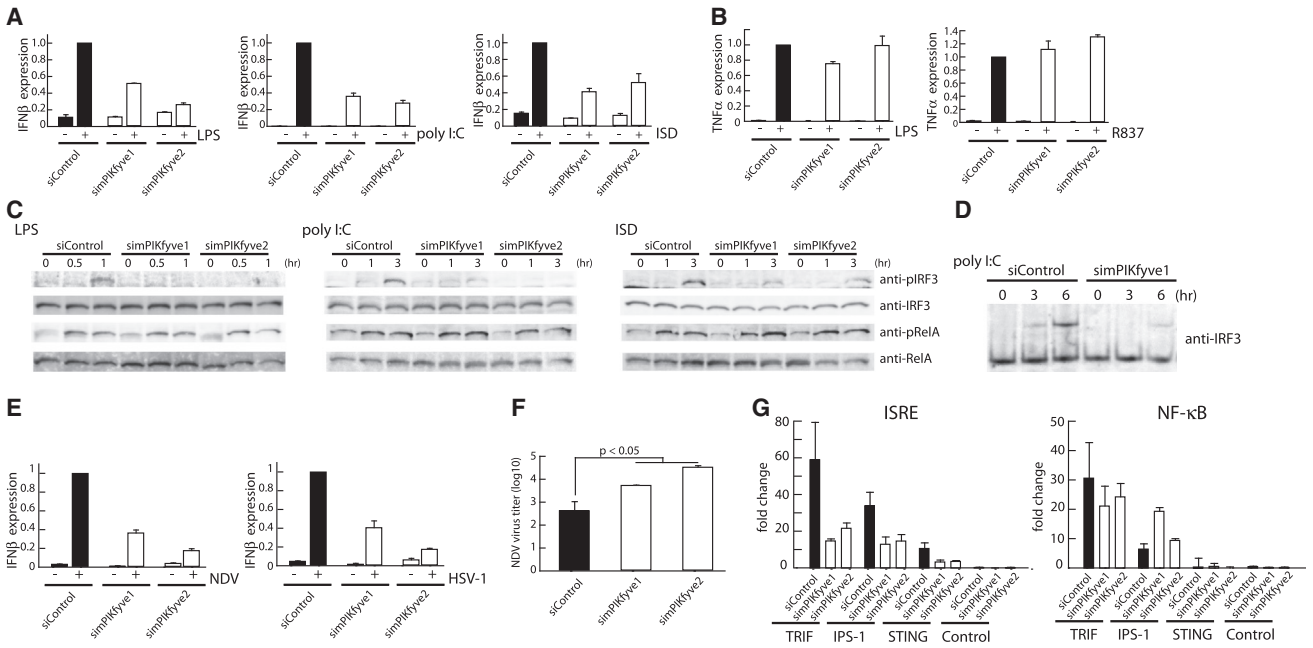

Figure 4. PIKfyve Knockdown Suppresses IFNβ Production by Reducing IRF3 Activation

(A–F) mPIKfyve knockdown by siRNA electroporation in MEF cells. (A) MEF cells were stimulated with LPS or transfected with poly(I:C), poly(dA:dT), or ISD, and expression of IFNβ mRNA was measured by qPCR. (B) Expression of TNF-α mRNA was quantified by qPCR after stimulation with LPS or R837. (C) MEF cells were stimulated with LPS or transfected with poly(I:C) or ISD, and immunoblotting was performed with the indicated antibodies. (D) IRF3 dimer formation was detected by native PAGE analysis. (E) MEF cells were infected with NDV or HSV-1, and expression of IFNβ mRNA was measured by qPCR. (F) MEF cells were infected with NDV at moi 0.1, and virus titer was measured after 24 hr by qPCR.

(G) hPIKfyve in HEK293 cells was knocked down by siRNA electroporation. ISRE or ELAM promoter plasmid was cotransfected with TRIF, IPS-1, or STING expression plasmid, and promoter activity was measured by luciferase assay. Data are represented as mean ± SD. Figure 4 is related to Figure S4.

suppressed by YM-201636 treatment, suggesting that PtdIns5P production from PIKfyve regulated substrate-kinase binding and phosphorylation. The kinase mutation in TBK1 also abrogated TBK1-IRF3 interactions, indicating that the interactions are mediated by its catalytic activity.

Interestingly, K360/R361 in hIRF3 is located in a cleft, termed the loop-helix region (LHR) pocket (Takahasi et al., 2003). To gain further insight into the mechanism of interaction, we simulated docking around the LHR pocket with the AutoDock4 and AutoDock Vina programs (Morris et al., 2009; Trott and Olson, 2010). Inositol1,5P_2, the inositol head of PtdIns5P, was used for the calculation, and docked conformations with a free phosphate group at position P1 were selected based on their energy (Figure 6F, Figures S5B and S5C). Both simulations provided very similar results. The docking result supported a model in which the inositol head of PtdIns5P is electrostatically stabilized by R361 in the LHR pocket and forms hydrogen bonds with the surrounding amino acids. Membrane surface interaction might be supported by dimer formation in order to enhance association (Figure S5D). In addition, based on the above results, K360 might be important for electrostatic interactions with the lipid membrane.

Cytokine Production and Adjuvant Effects of Synthetic C8-PtdIns5P

PIKfyve produces PtdIns5P from PtdIns and PtdIns3,5P2 from PtdIns3P by phosphorylation of the 5′ position in the inositol ring (Ikonomov et al., 2011; Sbrissa et al., 2002). To obtain direct evidence for PtdIns5P involvement in TBK1-IRF3 signaling, we investigated whether exogenous administration of synthetic PtdIns5P could induce cytokine production. Among the phosphatidylinositols phosphorylated at the 5′ position in the ring, treatment of GM-DCs with C8-PtdIns5P (a water-soluble lipid with a eight acyl chain) induced production of IP-10 and RANTES, but not IL-1β (Figure 7A and Figure S6A). In contrast, C8-PtdIns5P did not induce cytokine production from MEF or M-CSF-induced macrophages (Figure S6B and data not shown). Stimulation with water-insoluble C16 acyl chain phosphatidylinositol did not induce cytokine production (Figure S6C). To investigate whether production of these cytokines was mediated through the IRF3 signaling axis, we examined cytokine production in GM-DCs from IPS-1- or IRF3/IRF7-deficient mice. *Irf3* and *Irf7* gene expression partially compensate for each other and share PtdIns5P binding amino acids (Honda et al., 2006). Although wild-type and IPS-1 (MAVS)-deficient GM-DCs showed increased IP-10, RANTES, and IFNβ production following C8-PtdIns5P stimulation, IRF3/IRF7-deficient GM-DCs showed diminished production of these cytokines (Figure 7B). C8-PtdIns5P induced phosphorylation and dimer formation of IRF3 in GMDCs, but not Rel A phosphorylation (Figures S6D and S6E). Furthermore, C8-PtdIns5P treatment increased IFNα/β mRNA expression in MEF cells, but not in TBK1/IKKi-deficent MEF cells, suggesting C8-PtdIns5P-mediated activation requires TBK1/IKKi (Figure S6F). These results

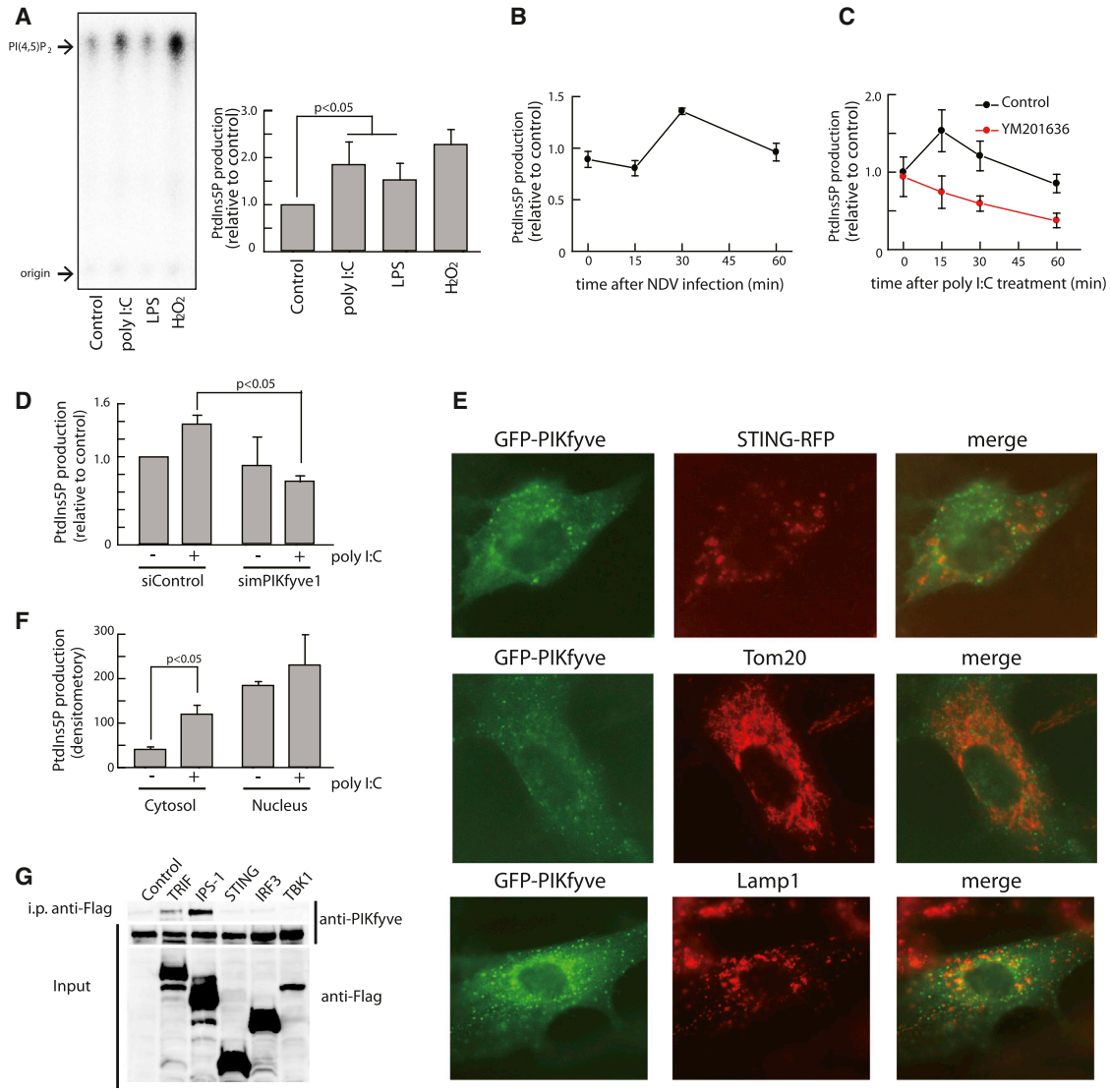

Figure 5. PtdIns5P Production Increases in MEF Cells after Stimulation

(A) The left panel shows the results of a representative PtdIns5P quantification experiment. PtdIns was isolated after stimulation using neomycin-coated beads, and PtdIns5P was converted to PtdIns4,5P_2 by PI5P4K in the presence of [gamma ^{32}P] ATP. PtdIns4,5P_2 was separated by TLC, and densitometry was measured. The bar graph shows mean densitometry values normalized to the control level.

(B–D) Time course of PtdIns5P production after NDV stimulation (moi 5) (B), poly(I:C) stimulation during YM-201636 treatment (C), or PIKfyve knockdown (D).

(E) MEF cells were cotransfected with GFP-PIKfyve and STING-RFP, and were stained with anti-Tom20 or anti-Lamp1.

(F) MEF cells were separated to cytosol and nucleus fraction, and PtdIns5P production was measured after PtdIns isolation.

(G) HEK293T cells were cotransfected with PIKfyve and indicated expression plasmid. Flag-tagged proteins were precipitated with anti-Flag agarose beads, and proteins were analyzed by immunoblotting using anti-PIKfyve or anti-Flag. Data are represented as mean ± SD.

indicated that PtdIns5P from PIKfyve targets TBK1/IKKi-IRF3/7 signal for cytokine production.

The cytokine production induced by C8-PtdIns5P in DCs prompted us to test whether C8-PtdIns5P acts as an adjuvant. C57BL/6J mice were immunized intramuscularly with ovalbumin (OVA) plus PBS, C8-PtdIns5P, or C8-PtdIns4,5P2 or were immunized intraperitoneally with OVA plus alum as a positive control, and after immunization OVA-specific total IgG in sera were measured. Mice immunized OVA and C8-PtdIns5P produced higher titers of OVA-specific IgG than did mice immunized with OVA and PBS or C8-PtdIns4,5P2 (Figure 7C). Increased levels of IgG1, but not other subclasses such as IgG2, IgG3, or IgA, were observed after four immunizations with C8-PtdIns5P (data not shown). The antigen-specific IgG production by PtdIns5P was diminished in IRF3/7-deficient mice, whereas the production by Alum was comparable between wild-type and IRF3/7-deficient mice (Figure 7D) (Marichal et al., 2011). Next, we investigated whether T cell activation was induced by PtdIns5P. In this regard, OVA-specific OT-II-transgenic CD4$^+$ T cells were cocultured with GM-DCs treated with C8-PtdIns5P,

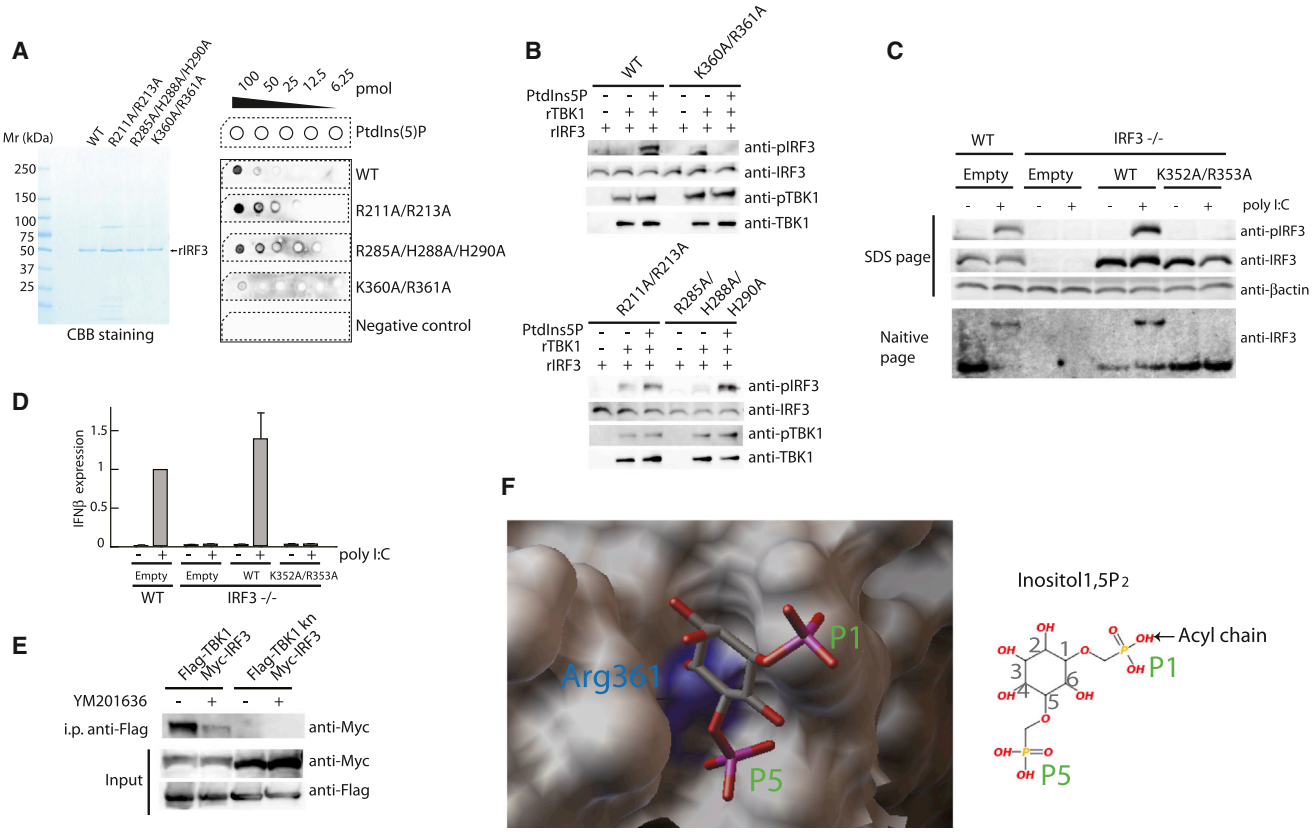

Figure 6. IRF3 Binding to PtdIns5P Is Critical for Signal Transduction

(A) Wild-type rIRF3 and mutant rIRF3 containing R211A/R213A, R285A/H288A/H290A, or K360A/R361A were purified and stained with Coomassie brilliant blue (CBB) after SDS-PAGE. Nitro cellulose membranes blotted with the indicated amount of PtdIns5P were incubated with the indicated proteins and binding proteins were detected by anti-IRF3.

(B) rIRF3 or mutant rIRF3 as subjected to in vitro kinase assay by incubation with PtdIns5P containing PC/PE liposomes.

(C and D) Wild-type MEF cells were infected with control retrovirus, and *IRF3*$^{-/-}$ MEF cells were infected with retrovirus expressing wild-type or K352A/R353A IRF3. (C) MEF cells were stimulated by poly(I:C) transfection, then immunoblotting was performed with the indicated antibodies, and IRF3 dimer formation was detected by native PAGE analysis. (D) Expression of IFNβ mRNA was measured by qPCR.

(E) HEK293T cells were transfected with IRF3 and TBK1 wild-type or TBK1 kinase negative (kn). Cells were treated with or without YM-201636, and binding protein to TBK1 was analyzed.

(F) (Left) Results of docking simulation with inositol1,5P_2 and IRF3 by Autodock vina are shown around LHR pocket. Blue indicates molecular surface of a side chain of Arg 361. (Right) Schematic representation of inositol1,5P_2 is shown by the same direction with the left. P1 site should be linked by acyl chain. Data are from one experiment represented of three (A, B, C, and E). Data are represented as mean ± SD (D). Figure 6 is related to Figure S5.

C8-PtdIns4,5P2, or poly(I:C) in the presence of OVA protein, and IFNγ production was measured (Figure 7E). C8-PtdIns5P treatment induced IFNγ production, whereas C8-PtdIns4,5P2 treatment did not. Therefore, these findings suggest that C8-PtdIns5P has an adjuvant-like property and induces antibody production through Th1 cell responses.

DISCUSSION

We showed that IFNβ induction through innate receptors is regulated by PtdIns5P, which targets the TBK1-IRF3 signaling axis. By in vitro kinase assay, IRF3 phosphorylation was barely detected, even in the presence of TBK1, whereas addition of PtdIns5P markedly induced IRF3 phosphorylation (Figure 1). These results suggest that phosphorylation sites on IRF3 are masked by other regions of IRF3 unless PtdIns5P is bound. Our docking simulation suggests that inositol1,5P_2, the head of PtdIns5P, fits into the LHR pocket of IRF3. In addition, the PLO assay demonstrates that R360 and R361 are necessary for binding to PtdIns5P (Figure 6). Therefore, we speculate that PtdIns5P binding may induce a conformational change in IRF3 to expose phosphorylation sites to which TBK1 gains access (Figure S6G).

Although PtdIns5P also binds to TBK1 in vitro, it does not affect TBK1 phosphorylation at S172. This suggests that PtdIns5P facilitates complex formation between TBK1 and IRF3, increasing the accessibility of TBK1 to IRF3, causing IRF3 phosphorylation in a proximal manner, but without affecting TBK1 activation. Alternatively, TBK1 S172 phosphorylation may not always reflect TBK1 activation during viral infection. Ubiquitination of TBK1 linked to K63 was reported to be an important modification for its activity (Li et al., 2011), suggesting that PtdIns5P binding to TBK1 may influence ubiquitination. Moreover, PtdIns5P binding to TBK1 may induce the recruitment of proteins such as TANK, NAP1, NEMO, and TRAF3, which

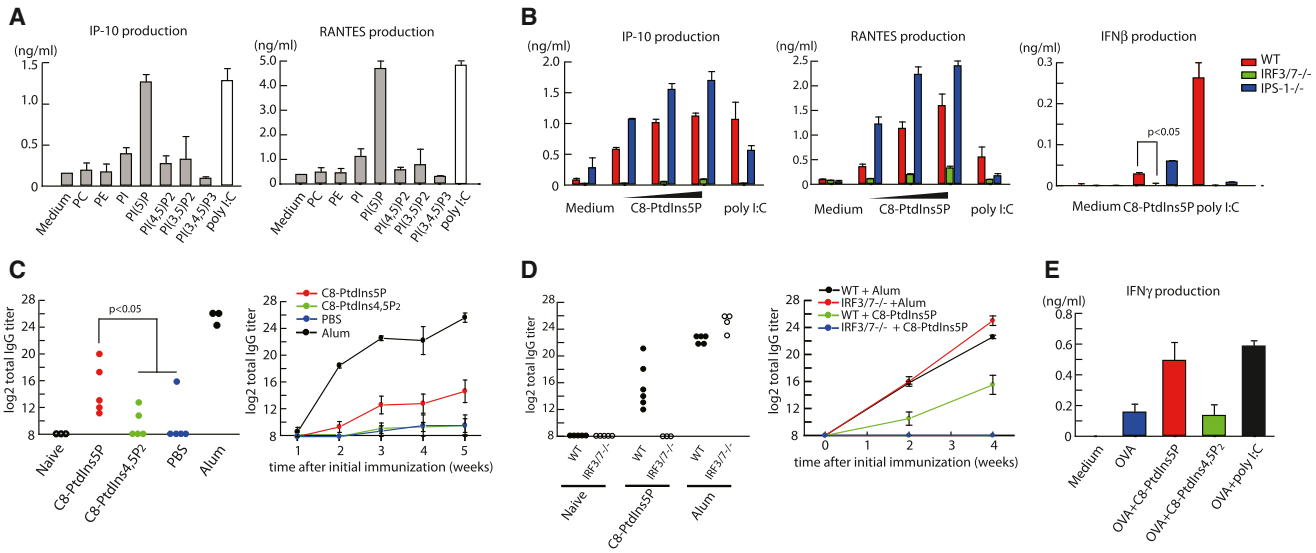

Figure 7. C8-PtdIns5P Induces Cytokine Production and Functions as an Adjuvant

(A) IP-10 and RANTES production from GM-DCs stimulated with the indicated C8-lipids were measured by ELISA.

(B) GM-DCs from wild-type, *IRF3*$^{-/-}$*/IRF7*$^{-/-}$ or *IPS-1 (MAVS)*$^{-/-}$ mice were stimulated with 10, 25, or 50 μM C8-PtdIns5P, and production of IP-10 and RANTES was analyzed by ELISA. GM-DCs were stimulated with C8-PtdIns5P for IFNβ measurement.

(C) Mice were immunized intramuscularly with ovalbumin (OVA) and PBS, or C8-PtdIns5P or C8-PtdIns4,5P2, or immunized intraperitoneally with OVA and alum as a positive control, and OVA-specific total IgG in sera was measured. IgG titers of each mouse was measured after 5 weeks (left). Time course analysis of IgG titers (right).

(D) Wild-type, *IRF3*$^{-/-}$*/IRF7*$^{-/-}$, or *IPS-1 (MAVS)*$^{-/-}$ mice were immunized intraperitoneally with OVA and alum, or intramuscularly immunized with OVA and C8-PtdIns5P. OVA-specific total IgG in sera was measured.

(E) OVA-specific OT-II-transgenic CD4^{+} T cells were isolated and cocultured with GM-DCs treated with C8-PtdIns5P, C8-PtdIns4,5P2, or poly(I:C) in the presence of OVA protein, and IFNγ production was measured. Data are represented as mean ± SD. Figure 7 is related to Figure S6.

regulate TBK1 activity downstream of TRIF, IPS-1, and STING (Bouwmeester et al., 2004; Fujita et al., 2003; Pomerantz and Baltimore, 1999; Ryzhakov and Randow, 2007; Tanaka and Chen, 2012).

PtdIns5P production is potentially mediated by several of the kinases and phosphatases listed in Figure 2A, but our results strongly suggest that innate immune signaling leads to PtdIns5P production by PIKfyve (Figure 5). Other kinases and phosphatases that mediate PtdIns5P production may play roles in distinct cellular signaling pathways (Figure S2A). For instance, although H_2O_2 stimulation increased PtdIns5P production (Figure 5A), it failed to produce type I IFN (data not shown). It was shown that H_2O_2 stimulation produces PtdIns5P in the nucleus by PI4K inhibition (Jones et al., 2006). PIKfyve localized in the cytosol and partially colocalized with STING-positive organelles and late endosomes. Production of PtdIns5P in organelles in the cytosol is likely to be important for TBK1-IRF3 signal transduction (Figure 5). The activation mechanism of PIKfyve have not been clearly understood so far, but PIKfyve might be activated by association with STING or other adaptor molecules in organelles for innate signaling.

PIKfyve can produce PtdIns3,5P_2 from PtdIns3P, a critical lipid for organelle trafficking (Ikonomov et al., 2011; Rutherford et al., 2006). It was suggested that in plasmacytoid DCs (pDCs), a subset of DCs that produce type I IFN upon viral infection via TLR7 or TLR9, PtdIns3,5P_2 is enriched in the endosome compartment where TLR9 is localized (Sasai et al., 2010). Therefore, we speculate that PIKfyve-dependent production of PtdIns3,5P_2 in pDCs plays important roles in virus infection-induced type I IFN by regulating TLR9 trafficking in pDCs.

We also found that synthetic-C8-PtdIns5P promotes production of cytokines such as IFNβ, IP-10, and RANTES, which are regulated by IRF3 (Figures 7A and 7B). Cytokine production by synthetic-C8-PtdIns5P, among several phosphatidylinositols, suggested that it was dependent on the phosphorylation site in the inositol head, and not on the acyl chain. In addition, the possibility of LPS contamination in synthetic C8-PtdIns5P was ruled out by the production of IP-10 in GM-DCs from *Tlr2*$^{-/-}$*/Tlr4*$^{-/-}$ mice (data not shown). Although the precise mechanisms underlying acyl length-specific cytokine production by PtdIns5P are not clear (Figures 7A and 7B and Figure S6B), the cellular incorporation rate of C8-PtdIns5P into GM-DCs may be appropriate for activation of TBK1-IRF3 signaling. Unlike poly(I:C), C8-PtdIns5P strongly induced IP-10 and RANTES and weakly induced IFNβ in GM-DCs. This suggests that in addition to IRF3 and IRF7, C8-PtdIns5P regulates unknown pathways required for IP-10 and RANTES induction. These findings suggested that *PIKfyve-PtdIns5P-TBK1-IRF3* signaling axis is activated in GM-DCs for the production of IFNβ. Although C8-PtdIns5P did not induce detectable amounts of IFNα/β in the protein level in MEF cells, it increased IFNα/β mRNA expression, which was diminished in TBK1/IKKi-deficient MEF cells (Figure S6F). Given that increased IFNβ mRNA was also found in MEFs, this axis is activated in MEF cells, but the signal activation

in MEF cells is weak as compared with in GM-DCs. This point should be clarified in the future.

C8-PtdIns5P also functions as an adjuvant in vivo that increases antigen-specific antibody production and $CD4^+$ T cell responses (Figures 7C–7E). At present, a remarkable number of ligands for PRRs have been discovered, some of them are being clinically tested, and European and U.S. licensing authorities have recommended that novel adjuvants be evaluated in nonclinical toxicology studies (Levitz and Golenbock, 2012). C8-PtdIns5P activates the TBK1-IRF3 signaling axis, suggesting that it could be useful as a new type of adjuvant.

EXPERIMENTAL PROCEDURES

Cells and Reagents

HEK293, HEK293T, and MEF cells were cultured in Dulbecco's modified Eagle's medium (DMEM) supplemented with 10% heat-inactivated fetal calf serum (FCS, Life Technologies) in a 5% CO_2 incubator. Preparation of MEF cells and generation of IPS-1-deficient and TBK1/IKKi-deficient MEF cells were described previously (Ishii et al., 2006; Kumar et al., 2006). GM-DCs were obtained from mouse bone marrow cells cultured in RPMI 1640 medium supplemented with 10% FCS, 100 μM 2-ME, and 10 ng/ml murine GM-CSF (BD Biosciences) for 6–8 days. LPS, poly(I:C), R837, and poly(dA:dT) were purchased from Invivogen, and DMXAA was purchased from Sigma. Sense and anti-sense ISD sequences were synthesized (Grainer Japan) and annealed (sense, 5′-TACAGATCTACTAGTGATCTATGACTGATCTGTACATGATCTACA). Poly(I:C) and poly(dA:dT) were mixed with Lipofectamine 2000 (Life Technologies) at a ratio of 2:1 (μg:μl) in OptiMEM (Life Technologies) for stimulation. C16-PtdIns, phosphatidylethanol, and PC were obtained from Avanti Polar Lipid, and C8-PtdIns was obtained from Echelon Biosciences. YM-201636, the PIKfyve inhibitor, was obtained from Santa Cruz. Antibodies were purchased from the following companies: anti-PIKfyve (Sigma), anti-pIRF3 (Cell Signaling), anti-pJNK (Cell Signaling), anti-TBK1 (Abcam), and anti-pTBK1 (Cell Signaling). ELISAs (R&D Systems) were performed according to the manufacturer's instructions.

Plasmid and Reporter Assay

The GFP-PIKfyve expression vector was a kind gift from Dr Tavaré (Hill et al., 2010). For construction of Flag-tagged PIKfyve, PIKfyve was amplified by PCR and ligated into pFLAG-CMV6 vector. A kinase-negative mutation at K1831M was introduced by KOD (Toyobo). Flag-tagged PIP5Kα, PIP5Kβ, and PIP5Kγ were amplified from HEK293 cDNA and cloned into a pFlag-CMV6 vector. PI3KIII, PTEN, TMEM55α, TMEM55β, and PI4K2α were obtained from a cDNA library cloned into a pCMV-SPORT6 vector (Open Biosystems). Flag-tagged IPS-1 and STING were described previously (Tsuchida et al., 2010). HEK293 cells were seeded onto 24-well plates and transfected with an expression plasmid and a luciferase reporter plasmid using Lipofectamine 2000 (Life Science Tech). After 16 hr, cells were lysed with passive lysis buffer (Promega), and luciferase activity was measured using the dual-luciferase reporter assay kit (Promega). The reporter plasmid for IFNβ and ISRE was described previously (Tsuchida et al., 2010). NF-κB activation was determined by the ELAM- or NF-κB-luc reporter assay. TK promoter-driven Renilla luciferase plasmid was used as an internal control.

In Vitro Phosphorylation

GST-tagged IRF3 was purified from *Escherichia coli*, and tags were eliminated using precision protease (BD Biosciences) according to the manufacturer's instructions. GST-TBK1 was purified from HEK293T cells and eluted in 10 mM glutathione. For the in vitro kinase assay, 20 ng of TBK1 and 100 nmol of IRF3 were incubated in reaction buffer (10 μM ATP, 100 mM NaCl, 2 mM $MgCl_2$, 5 mM HEPES [pH 7.2]) at 30°C for 30 min. Liposomes were formed at a ratio PC:PE:PI of 30:8:2 in reaction buffer by sonication and subjected to in vitro kinase assay at 40 μM. GST-tagged STING was expressed in HEK293T cells and purified using glutathione Sepharose beads. Purified STING was reconstituted in azolectin lipid membrane by forming liposomes under dialysis. Lipid separation was then performed.

Protein Lipid Overlay Assay

Purified IRF3 or GST-TBK1 proteins (100 nM) were incubated with membrane lipid strips (Echelon Biosciences) or Hybond-C membrane (Amersham Biosciences) spotted PtdIns5P in TBST buffer (140 mM NaCl, 2.5 mM KCl, 25 mM Tris [pH 8.0], 0.05% Tween 20). Membranes were washed three times with TBST and incubated with anti-IRF3 or anti-TBK1, then further incubated with secondary antibody for development.

Immunoprecipitation

RAW264.7 cells were lysed in lysis buffer (150 mM NaCl, 10 mM EGTA, 2 mM EDTA, 25 mM Tris [pH 8.0], 0.1% NP40) after stimulation, and TBK1 was precipitated by anti-TBK1 with IgA agarose beads (GE Healthcare) for 3 hr at 4°C. Beads were washed three times, and bound proteins were separated by SDS-PAGE.

siRNA and Quantitative RT-PCR

The target sequence for mouse PIKfyve is simPIKfyve1, 5′-UAAAUAAGGACUCUUUGAUGAAGGC-3′ (sense) simPIKfyve2; and 5′-UCAGAAGGUUUCACAGGUGUACCUA-3′ (sense) (Life Science Technology). The target sequence for human PIKfyve is sihPIKfyve1, 5′-UGAUUUGCCUCGAUCUCCUUU-3′ (sense); and sihPIKfyve2, 5′-AAAUCUCCUGCUCGAAAUAUU-3′ (sense) (Greiner). siRNA was electroporated by NEON (Life Technologies). Two days after electroporation, MEF and HEK293 cells were stimulated with various reagents or virus. Total RNA was isolated using Trizol reagent (Life Technologies) and reverse transcribed by ReverTraAce (Toyobo) according to the manufacturer's instructions. Real-time PCR was performed using the following primers: mIFNβ, sense 5′-ATGGTGGTCCGAGCAGAGAT-3′, reverse 5′-CCACCACTCATTCTGAGGCA-3′; mIP-10, sense 5′-CCATCAGCACCATGAACCCAAGT-3′, reverse 5′-CACTCCAGTTAAGGAGCCCTTTTAGACC-3′; mRANTES, sense 5′- CTCACCATATGGCTCGGACA-3′, reverse 5′-ACAAACACGACTGCAAGATTGG-3′; mGAPDH, sense 5′-TGACGTGCCGCCTGGAGAAA-3′, reverse 5′-AGTGTAGCCCAAGATGCCCTTCAG-3′; mIL-6, sense 5′-GTAGCTATGGTACTCCAGAAGAC-3′, reverse 5′-ACGATGATGCACTTGCAGAA-3′; and mPIKfyve, sense 5′- AAGTCTTACCCTCACATGAGCTAGTGA-3′, reverse 5′- ATCAGCTAGCATTCTACCCAAGGT-3′. hPIKfyve, sense 5′-TGGATGCCAGATAGCCAATGT-3′, reverse 5′-TGTCTGCGCCTAAAGGTTGTAAA-3′.

PtdIns5P Mass Assay

A PtdIns5P conversion assay was performed as described by Morris et al. (Morris et al., 2000). Briefly, PtdIns including PtdIns5P were isolated, and the amount of PtdIns5P was detected by ^{32}P incorporation by forming $PtdIns4,5P_2$ in an in vitro kinase assay. Cells were seeded onto 6-well plates at a density of 2×10^5 cells per well. After stimulation, cells were collected and lipids were isolated using chloroform/methanol (1:1; v/v). Total PtdIns were further isolated using neomycin-coated glass beads prepared according to previously reported procedures (Schacht, 1978) using glycerol controlled pore glass (Sigma). Lipid extracts were incubated with 20 μl of packed neomycin beads for 20 min in AF buffer (chloroform/methanol/330 mM ammonium formate [5:10:1; v/v]), and beads were washed twice with AF buffer. Bound PtdIns were eluted by chloroform/methanol/2.4 M HCl (5:10:4; v/v). Eluted samples were exchanged in chloroform buffer and dried by SpeedVac at a low/medium heat setting for 30 min after addition of 5 nmols of phosphatidylserine and 1.5 nmols of phosphatidic acid as a carrier. Dried PtdIns were suspended in 40 μl of kinase assay buffer (80 mM KCl, 50 mM Tris [pH 7.4], 10 mM $MgCl_2$, 2 mM EGTA) by sonication, and a PtdIns conversion assay was started by incubation with 0.1 μg of bacterially expressed PI4KIIα for 2 hr at 30°C in the presence of [gamma ^{32}P] ATP. PI4KIIα was subcloned in a pGEX vector (GE Healthcare), and recombinant protein was purified from *E. coli*. The reaction was terminated by addition of 200 μl of 1 M HCl, and protein was extracted with 160 μl of chloroform/methanol (1:1; v/v). The lower layers were washed twice with 100 μl of methanol/1 M HCl (1:1; v/v), and phosphorylated PtdIns5P ($Ptd4,5P_2$) was separated by thin-layer chromatography (TLC). Then 15 μl of the lower layers was spotted onto a TLC silica plate (GE Healthcare) and separated by chloroform/methanol/5.6% ammonium in water (45:35:10; v/v). The TLC plate was dried and developed on an imaging plate, and ^{32}P densitometries were counted using a Typhoon FLA7000 system (Fuji Film).

Docking Simulation

Ins1,5P_2 ligand was created from the Ins1,4,5P_3 ligand, and 1J2F (Takahasi et al., 2003) was used as a receptor. The hydrogen positions and Gasteiger charges were calculated by Autodock tools. The Autodock4 (Morris et al., 2009) and Autodock vina (Trott and Olson, 2010) programs were run using default parameters.

Mouse Immunization

*IPS-1*deficient (*Mavs*)$^{-/-}$, *Irf3*$^{-/-}$/*Irf7*$^{-/-}$, and OT-II mice have been described previously (Kumar et al., 2006; Uematsu et al., 2008). All animal experiments were performed with the approval of the Animal Research Committee of the Research Institute for Microbial Diseases at Osaka University. For mice immunizations, C57BL/6J mice (Japan Clea) were immunized intraperitoneally with 100 μg of OVA (Seikagaku Corporation) and 1 mg of alum (Sigma) or immunized intramuscularly with 100 μg of OVA/100 μg of C8-PtdIns every week for a total of four immunizations. C8-PtdIns5P and C8-PtdIns4,5P_2 were solubilized in PBS and mixed with OVA for immunization. For coculture experiments, 1 × 10^5 OVA-specific OT-II-transgenic CD4$^+$ T cells and 1 × 10^5 GM-DCs treated with C8-PtdIns5P, C8-PtdIns4,5P_2 or poly(I:C) were cultured in the presence of 10 μg of OVA protein for 7 days, and IFNγ production was measured.

Statistics

Statistical significance was determined by Student's t test. A p value of <0.05 was considered significant.

SUPPLEMENTAL INFORMATION

Supplemental Information includes six figures and can be found with this article online at http://dx.doi.org/10.1016/j.chom.2013.07.011.

ACKNOWLEDGMENTS

We are grateful to K. Ohata and S. Uematsu for helpful discussion. We also thank all lab members, especially M. Nishino, N. Kitagaki, and C. Funamoto, for their technical assistance, and E. Kamada and M. Kageyama for their secretarial assistance. This study was supported by a KAKENHI Grant-in-Aid for Research Activity (B) (23790296) and (A) (23689030). This study was also supported by basic research grant from the National Institutes of Health (NIH AI070167-06A1) and the Special Coordination Funds of the Japanese Ministry of Education, Culture, Sports, Science, and Technology, as well as the Ministry of Health, Labour, and Welfare in Japan and the Japan Society for the Promotion of Science through the Funding Program for World-Leading Innovative R&D on Science and Technology (FIRST Program). D.M.S. acknowledges additional support from the Platform for Drug Discovery, Informatics, and Structural Life Science from the Ministry of Education, Culture, Sports, Science, and Technology, Japan.

Received: January 28, 2013
Revised: May 17, 2013
Accepted: July 16, 2013
Published: August 14, 2013

REFERENCES

Berger, K.L., and Randall, G. (2009). Potential roles for cellular cofactors in hepatitis C virus replication complex formation. Commun. Integr. Biol. *2*, 471–473.

Bouwmeester, T., Bauch, A., Ruffner, H., Angrand, P.O., Bergamini, G., Croughton, K., Cruciat, C., Eberhard, D., Gagneur, J., Ghidelli, S., et al. (2004). A physical and functional map of the human TNF-alpha/NF-kappa B signal transduction pathway. Nat. Cell Biol. *6*, 97–105.

Clark, K., Plater, L., Peggie, M., and Cohen, P. (2009). Use of the pharmacological inhibitor BX795 to study the regulation and physiological roles of TBK1 and IkappaB kinase epsilon: a distinct upstream kinase mediates Ser-172 phosphorylation and activation. J. Biol. Chem. *284*, 14136–14146.

Clark, K., Takeuchi, O., Akira, S., and Cohen, P. (2011). The TRAF-associated protein TANK facilitates cross-talk within the IkappaB kinase family during Toll-like receptor signaling. Proc. Natl. Acad. Sci. USA *108*, 17093–17098.

Fitzgerald, K.A., McWhirter, S.M., Faia, K.L., Rowe, D.C., Latz, E., Golenbock, D.T., Coyle, A.J., Liao, S.M., and Maniatis, T. (2003). IKKepsilon and TBK1 are essential components of the IRF3 signaling pathway. Nat. Immunol. *4*, 491–496.

Fujita, F., Taniguchi, Y., Kato, T., Narita, Y., Furuya, A., Ogawa, T., Sakurai, H., Joh, T., Itoh, M., Delhase, M., et al. (2003). Identification of NAP1, a regulatory subunit of IkappaB kinase-related kinases that potentiates NF-kappaB signaling. Mol. Cell. Biol. *23*, 7780–7793.

Guiducci, C., Ghirelli, C., Marloie-Provost, M.A., Matray, T., Coffman, R.L., Liu, Y.J., Barrat, F.J., and Soumelis, V. (2008). PI3K is critical for the nuclear translocation of IRF-7 and type I IFN production by human plasmacytoid predendritic cells in response to TLR activation. J. Exp. Med. *205*, 315–322.

Hill, E.V., Hudson, C.A., Vertommen, D., Rider, M.H., and Tavaré, J.M. (2010). Regulation of PIKfyve phosphorylation by insulin and osmotic stress. Biochem. Biophys. Res. Commun. *397*, 650–655.

Honda, K., Takaoka, A., and Taniguchi, T. (2006). Type I interferon [corrected] gene induction by the interferon regulatory factor family of transcription factors. Immunity *25*, 349–360.

Hrincius, E.R., Dierkes, R., Anhlan, D., Wixler, V., Ludwig, S., and Ehrhardt, C. (2011). Phosphatidylinositol-3-kinase (PI3K) is activated by influenza virus vRNA via the pathogen pattern receptor Rig-I to promote efficient type I interferon production. Cell. Microbiol. *13*, 1907–1919.

Ikonomov, O.C., Sbrissa, D., Delvecchio, K., Xie, Y., Jin, J.P., Rappolee, D., and Shisheva, A. (2011). The phosphoinositide kinase PIKfyve is vital in early embryonic development: preimplantation lethality of PIKfyve−/− embryos but normality of PIKfyve+/− mice. J. Biol. Chem. *286*, 13404–13413.

Ishii, K.J., Coban, C., Kato, H., Takahashi, K., Torii, Y., Takeshita, F., Ludwig, H., Sutter, G., Suzuki, K., Hemmi, H., et al. (2006). A Toll-like receptor-independent antiviral response induced by double-stranded B-form DNA. Nat. Immunol. *7*, 40–48.

Ishii, K.J., Kawagoe, T., Koyama, S., Matsui, K., Kumar, H., Kawai, T., Uematsu, S., Takeuchi, O., Takeshita, F., Coban, C., and Akira, S. (2008). TANK-binding kinase-1 delineates innate and adaptive immune responses to DNA vaccines. Nature *451*, 725–729.

Jefferies, H.B., Cooke, F.T., Jat, P., Boucheron, C., Koizumi, T., Hayakawa, M., Kaizawa, H., Ohishi, T., Workman, P., Waterfield, M.D., and Parker, P.J. (2008). A selective PIKfyve inhibitor blocks PtdIns(3,5)P(2) production and disrupts endomembrane transport and retroviral budding. EMBO Rep. *9*, 164–170.

Jones, D.R., Bultsma, Y., Keune, W.J., Halstead, J.R., Elouarrat, D., Mohammed, S., Heck, A.J., D'Santos, C.S., and Divecha, N. (2006). Nuclear PtdIns5P as a transducer of stress signaling: an in vivo role for PIP4Kbeta. Mol. Cell *23*, 685–695.

Kawai, T., and Akira, S. (2011). Toll-like receptors and their crosstalk with other innate receptors in infection and immunity. Immunity *34*, 637–650.

Kishore, N., Huynh, Q.K., Mathialagan, S., Hall, T., Rouw, S., Creely, D., Lange, G., Caroll, J., Reitz, B., Donnelly, A., et al. (2002). IKK-i and TBK-1 are enzymatically distinct from the homologous enzyme IKK-2: comparative analysis of recombinant human IKK-i, TBK-1, and IKK-2. J. Biol. Chem. *277*, 13840–13847.

Kondo, T., Kobayashi, J., Saitoh, T., Maruyama, K., Ishii, K.J., Barber, G.N., Komatsu, K., Akira, S., and Kawai, T. (2013). DNA damage sensor MRE11 recognizes cytosolic double-stranded DNA and induces type I interferon by regulating STING trafficking. Proc. Natl. Acad. Sci. USA *110*, 2969–2974.

Koyasu, S. (2003). The role of PI3K in immune cells. Nat. Immunol. *4*, 313–319.

Kumar, H., Kawai, T., Kato, H., Sato, S., Takahashi, K., Coban, C., Yamamoto, M., Uematsu, S., Ishii, K.J., Takeuchi, O., and Akira, S. (2006). Essential role of IPS-1 in innate immune responses against RNA viruses. J. Exp. Med. *203*, 1795–1803.

Levitz, S.M., and Golenbock, D.T. (2012). Beyond empiricism: informing vaccine development through innate immunity research. Cell *148*, 1284–1292.

Li, S., Wang, L., Berman, M., Kong, Y.Y., and Dorf, M.E. (2011). Mapping a dynamic innate immunity protein interaction network regulating type I interferon production. Immunity *35*, 426–440.

Marichal, T., Ohata, K., Bedoret, D., Mesnil, C., Sabatel, C., Kobiyama, K., Lekeux, P., Coban, C., Akira, S., Ishii, K.J., et al. (2011). DNA released from dying host cells mediates aluminum adjuvant activity. Nat. Med. *17*, 996–1002.

Morris, J.B., Hinchliffe, K.A., Ciruela, A., Letcher, A.J., and Irvine, R.F. (2000). Thrombin stimulation of platelets causes an increase in phosphatidylinositol 5-phosphate revealed by mass assay. FEBS Lett. *475*, 57–60.

Morris, G.M., Huey, R., Lindstrom, W., Sanner, M.F., Belew, R.K., Goodsell, D.S., and Olson, A.J. (2009). AutoDock4 and AutoDockTools4: automated docking with selective receptor flexibility. J. Comput. Chem. *30*, 2785–2791.

Pendaries, C., Tronchère, H., Arbibe, L., Mounier, J., Gozani, O., Cantley, L., Fry, M.J., Gaits-Iacovoni, F., Sansonetti, P.J., and Payrastre, B. (2006). PtdIns5P activates the host cell PI3-kinase/Akt pathway during Shigella flexneri infection. EMBO J. *25*, 1024–1034.

Pomerantz, J.L., and Baltimore, D. (1999). NF-kappaB activation by a signaling complex containing TRAF2, TANK and TBK1, a novel IKK-related kinase. EMBO J. *18*, 6694–6704.

Qin, B.Y., Liu, C., Lam, S.S., Srinath, H., Delston, R., Correia, J.J., Derynck, R., and Lin, K. (2003). Crystal structure of IRF-3 reveals mechanism of autoinhibition and virus-induced phosphoactivation. Nat. Struct. Biol. *10*, 913–921.

Rutherford, A.C., Traer, C., Wassmer, T., Pattni, K., Bujny, M.V., Carlton, J.G., Stenmark, H., and Cullen, P.J. (2006). The mammalian phosphatidylinositol 3-phosphate 5-kinase (PIKfyve) regulates endosome-to-TGN retrograde transport. J. Cell Sci. *119*, 3944–3957.

Ryzhakov, G., and Randow, F. (2007). SINTBAD, a novel component of innate antiviral immunity, shares a TBK1-binding domain with NAP1 and TANK. EMBO J. *26*, 3180–3190.

Sancho, D., and Reis e Sousa, C. (2012). Signaling by myeloid C-type lectin receptors in immunity and homeostasis. Annu. Rev. Immunol. *30*, 491–529.

Sasai, M., Linehan, M.M., and Iwasaki, A. (2010). Bifurcation of Toll-like receptor 9 signaling by adaptor protein 3. Science *329*, 1530–1534.

Sbrissa, D., Ikonomov, O.C., Deeb, R., and Shisheva, A. (2002). Phosphatidylinositol 5-phosphate biosynthesis is linked to PIKfyve and is involved in osmotic response pathway in mammalian cells. J. Biol. Chem. *277*, 47276–47284.

Schacht, J. (1978). Purification of polyphosphoinositides by chromatography on immobilized neomycin. J. Lipid Res. *19*, 1063–1067.

Strowig, T., Henao-Mejia, J., Elinav, E., and Flavell, R. (2012). Inflammasomes in health and disease. Nature *481*, 278–286.

Sun, L., Wu, J., Du, F., Chen, X., and Chen, Z.J. (2013). Cyclic GMP-AMP synthase is a cytosolic DNA sensor that activates the type I interferon pathway. Science *339*, 786–791.

Takahasi, K., Suzuki, N.N., Horiuchi, M., Mori, M., Suhara, W., Okabe, Y., Fukuhara, Y., Terasawa, H., Akira, S., Fujita, T., and Inagaki, F. (2003). X-ray crystal structure of IRF-3 and its functional implications. Nat. Struct. Biol. *10*, 922–927.

Tanaka, Y., and Chen, Z.J. (2012). STING specifies IRF3 phosphorylation by TBK1 in the cytosolic DNA signaling pathway. Sci. Signal. *5*, ra20.

Trott, O., and Olson, A.J. (2010). AutoDock Vina: improving the speed and accuracy of docking with a new scoring function, efficient optimization, and multithreading. J. Comput. Chem. *31*, 455–461.

Tsuchida, T., Zou, J., Saitoh, T., Kumar, H., Abe, T., Matsuura, Y., Kawai, T., and Akira, S. (2010). The ubiquitin ligase TRIM56 regulates innate immune responses to intracellular double-stranded DNA. Immunity *33*, 765–776.

Uematsu, S., Fujimoto, K., Jang, M.H., Yang, B.G., Jung, Y.J., Nishiyama, M., Sato, S., Tsujimura, T., Yamamoto, M., Yokota, Y., et al. (2008). Regulation of humoral and cellular gut immunity by lamina propria dendritic cells expressing Toll-like receptor 5. Nat. Immunol. *9*, 769–776.

Wilcox, A., and Hinchliffe, K.A. (2008). Regulation of extranuclear PtdIns5P production by phosphatidylinositol phosphate 4-kinase 2alpha. FEBS Lett. *582*, 1391–1394.